Catena 181 (2019) 104061

Contents lists available at ScienceDirect

Catena

journal homepage: www.elsevier.com/locate/catena

Tropical forest structure and understorey determine subsurface flow through biopores formed by plant roots

Jérôme Nespoulous[a], Luis Merino-Martín[a,b], Yogan Monnier[a], Diane C. Bouchet[a], Merlin Ramel[a], Rodolphe Dombey[a], Gaelle Viennois[a], Zhun Mao[a], Jiao-Lin Zhang[c], Kun-Fang Cao[d], Yves Le Bissonnais[e], Roy C. Sidle[f,g], Alexia Stokes[a,*]

[a] AMAP, INRA, CIRAD, IRD, CNRS, University of Montpellier, Montpellier, France
[b] CEFE, CNRS, Univ. Montpellier, Univ. Paul Valéry Montpellier 3, EPHE, IRD, Montpellier, France
[c] Key Laboratory of Tropical Forest Ecology, Xishuangbanna Tropical Botanical Garden, Chinese Academy of Sciences, Mengla, Yunnan 666303, China
[d] State Key Laboratory College of Forestry for Conservation and Utilization of Subtropical Agro-bioresources, Guangxi University, Nanning, Guangxi 530004, China
[e] INRA, UMR LISAH, F-34060 Montpellier, France
[f] University of Sunshine Coast, Sustainability Research Centre, Sippy Downs, Queensland, Australia
[g] Mountain Societies Research Institute, University of Central Asia, Khorog GBAO, Tajikistan

ARTICLE INFO

Keywords:
Brilliant Blue
Ferralsol
Hevea brasiliensis
Mass wasting processes
Preferential flow
Root density mapping

ABSTRACT

Erosion and mass wasting processes on mountain slopes can benefit from or be adversely affected by the presence of biopores formed by plant root systems or soil fauna. The relationship between biopores and subsurface flow during rainstorms is poorly understood. Here, we examined the link between subsurface flow and biopores formed through different processes, including soil faunal activity and abundance of fine and coarse roots. As the distribution of biopores is influenced by the type of vegetation present, we investigated the effect of plant diversity (forest with or without understorey vegetation) on the pattern of water infiltration throughout the soil. We hypothesized that increased species diversity would enhance the extension of subsurface flow because biopores would be distributed throughout the soil profile and that more coarse roots would create large biopores, increasing subsurface flow. In situ experiments were conducted on hillslopes with plantations of rubber trees (*Hevea brasiliensis*) growing on terraces, or with secondary mixed forests, in the tropical zone of Yunnan province, China. Three sites with Ferralsol soils and different vegetation types were examined: (1) plantation with no understorey; (2) clear-cut plantation with understorey; and (3) secondary mixed forest with understorey. Irrigation experiments with Brilliant Blue FCF dyed water were performed upslope of trees at each site and staining patterns resulting from infiltrated dyed water were examined at two different scales. After dye irrigation, soil was removed in 1.0 × 0.8 m slices starting 1 m downslope and soil profiles were photographed for subsequent mapping of dyed areas in the profile (macroscale). Each profile was then divided into a 0.1 × 0.1 m grid (microscale) and burrows formed by macrofauna and fine and coarse root densities were measured. At the macroscale, the greatest lateral extension in subsurface flow occurred in the natural forest and the least in the rubber tree plantation with no understorey vegetation. At the microscale, and in all types of vegetation, fine roots significantly increased the incidence of subsurface flow compared to coarse roots and macrofauna activity. We conclude that in tropical Ferralsols, fine roots, and hence understorey vegetation, play a positive role in promoting subsurface flow and therefore reducing water erosion and mass wasting processes. Thus, planting mixtures that include a diversity of species and strata could significantly improve soil conservation.

1. Introduction

Water erosion and mass wasting processes, such as shallow landslides, are recurring problems around the world (Sidle and Ochiai, 2006; Stokes et al., 2013), notably in mountainous areas that are particularly vulnerable to anthropogenic pressure and global change (Elkin et al., 2013). In Southeast Asia, and China in particular, soil degradation on steep slopes has been accelerated during the last 50 years, due to poor farming practices, deforestation, road and dam construction (Sidle et al., 2006; Stokes et al., 2010; Sidle et al., 2014).

* Corresponding author.
E-mail address: alexia.stokes@cirad.fr (A. Stokes).

https://doi.org/10.1016/j.catena.2019.05.007
Received 3 July 2018; Received in revised form 22 March 2019; Accepted 4 May 2019
Available online 05 June 2019

The conversion of large swathes of tropical rainforest to rubber tree (*Hevea brasiliensis* Mull. Arg.) plantations has also led to major soil erosion and concerns about water cycling (Ziegler et al., 2009; Ahrends et al., 2015; Häuser et al., 2015). In steep areas, the frequent practice of constructing bench terraces before planting rubber trees changes soil physical and hydrological properties: (i) soil in the bench terraces is destabilized by excavation and terrace construction (Sidle et al., 2006), and (ii) herbicides are used to remove understorey vegetation and the unvegetated riser faces are more vulnerable to surface erosion than the original slope (van Dijk, 2002; Liu et al., 2015). Terraces need constant maintenance and after forest operations such as clear-felling, they are susceptible to failure because of changes in hydrological regime, such as an increase of the heterogeneity of infiltration and wetting front (Fredlund et al., 2012), which correspond to vertical macropore flow towards the potential slip plane (Cammeraat et al., 2005), or increases in the weight of soil water (overburden effect). Therefore, to better manage soil conservation in rubber tree plantations, it is necessary to understand how water moves through soil along natural and terraced slopes.

Hydrological and mass wasting processes on vegetated slopes are influenced by soil structure and plant root system morphology (Sidle and Ochiai, 2006). Water flows through two domains within soils (Alaoui, 2006): (i) soil matrix flow, consisting of both uniform saturated and unsaturated flow through fine pores and (ii) uniform and non-uniform preferential flow, occurring inside of single or interconnected systems of macropores with diameters > 2 mm, although preferential flow can also occur in more narrow pores (Tsuboyama et al., 1994; Sidle et al., 2001). If the macropores are not maintained by live roots, fauna or the frequent passage of water, they gradually disappear and become “invisible pores”, or mesopores, but are still very permeable and contribute significantly to preferential flow (Tsukamoto and Ohta, 1988). Biotic macropores (or biopores, Fig. S1) include root channels (Mitchell et al., 1995), particularly large diameter (coarse) roots (Bodner et al., 2014) and faunal burrows (Noguchi et al., 1997a; Farenhorst et al., 2000; Shuster et al., 2002; Weiler and Naef, 2003), while non-biotic macropores are formed by freeze-thaw, wetting-drying, dissolution of soil materials, physicochemical soil aggregation, and subsurface erosion (Aubertin, 1971). Root systems can create stable channels when growing in the soil, largely through: (i) compression of soil particles as the root penetrates the soil and (ii) amalgamation of soil particles with sloughed root cells and mucilage (Bengough et al., 1997). Both live and dead plant roots can promote slope drainage by functioning as hillslope-scale subsurface flow paths that drain subsurface water away from potentially unstable sites (Noguchi et al., 1999, 2001). Conversely, when root channels converge or when subsurface flow abruptly terminates in the slope (e.g., dead-end channels), water pressure may concentrate in critical zones of the slope, thus promoting instability. Therefore, flow paths can exert both positive and negative consequences on slope stability (Ghestem et al., 2011; Sidle and Bogaard, 2016). The effects of different land-use types on water flows in soil have been studied with a focus on soil hydraulic properties related to matrix flow (Schwartz et al., 2003; Bodhinayake and Cheng Si, 2004; Bormann and Klaassen, 2008; Wu et al., 2017) more than preferential flow (Vogel et al., 2006). It is not well known how different types of vegetation and land-use influence preferential flow paths and especially how root morphology and pedofaunal activity affect the formation, density and diameter of biopores.

Recently, Jiang et al. (2017, 2018) studied patterns of water infiltration through soil in rubber tree plantations in Yunnan, China, using a single infiltration cylinder (with a diameter of 0.2 m). Although infiltration was greater in rooted soil compared to bare soil, the effects of preferential flow in biopores and matrix flow (in pores < 2 mm in diameter) could not be distinguished. In particular, the impact of coarse roots (> 2 mm in diameter) cannot be determined with small diameter infiltration cylinders because of scaling and edge effects (Ghestem et al., 2011; Zhang et al., 2017; Sidle et al., 2017). Coarse roots are thought to play a major, but poorly understood role, in preferential flow processes (Lange et al., 2009; Ghestem et al., 2011) but few field data are available to quantify the effect (Wang and Zhang, 2017).

We explored the mechanisms through which root systems and soil macrofauna play a role on subsurface flow processes along forested hillslopes in Yunnan, China. We hypothesized that: (i) natural, mixed forests would have a greater extension of subsurface flow compared to monospecific rubber tree plantations, because biopores should be distributed throughout the entire soil profile, due to the increased diversity of macrofauna and plant species and their different root system morphologies, and (ii) a greater number of coarse roots would increase subsurface flow. To understand the processes occurring, two different scales were considered: the pattern of water infiltration throughout the soil profile, which reflected the impact of vegetation type on subsurface flow (macroscale) and a finer ‘microscale,’ whereby the effects of the density and size of individual roots and burrows on infiltration were elucidated.

2. Materials and methods

2.1. Study sites

Study sites were located on the Nan Lin Shan mountain of Xishuangbanna, Yunnan province, China. All sites were located on slopes around Bashayicun village (21°56′31.70″N; 100°50′49.60″E), 10 km south of Jinghong in the Mekong catchment. The climate is tropical with a mean annual temperature of 24.7 °C and mean annual precipitation of 1145 mm (mean values for the period 2013–2015 in Jinghong), with 82% of precipitation occurring during the monsoon season. Slope gradient ranged from 30° to 40° and all sites were situated at an altitude of about 800 m. In this region, soil surface erosion is severe and numerous landslides occur, usually on farmed slopes or in rubber tree (*Hevea brasiliensis* (Willd. ex A. Juss. Müll. Arg.) plantations, during the monsoon season (May–September).

2.2. Vegetation types

Three sites were chosen within a landscape dominated by rubber tree plantations (Fig. 1). All sites were close together and similarly oriented: i) ‘*plantation*’ corresponding to a 0.45 ha rubber tree stand. Soil between tree lines was largely bare as some leaf litter was observed during the autumn and herbicides were regularly used to kill herbaceous vegetation, ii) ‘*clear-cut*’ comprising a 0.41 ha site where rubber trees were felled in 2011. One year after this felling, young rubber trees were planted as rootstock, with one plant beside each remaining tree stump. Herbaceous vegetation was also present, that was colonizing the recently exposed soil (Table 1), and iii) ‘*forest*’ which consisted of mixed secondary forest without any associated crops (Fig. 1). A diversity of tree species, shrubs, grass and litter was present at the forest site (Table 1); total tree density was 11,795 trees ha^{-1} within the entire 7 ha *forest* site.

Rubber tree plantations (*plantation* and *clear-cut* sites) were grown on man-made terraces (with a ‘cut’ slope about 0.8 m high and with a distance between terraces that was about 2.0 m wide). Although the terraces may have different slope morphologies compared to the *forest* site, and thus have altered soil structural properties, both *plantation* and *clear-cut* had the same type of terraces and so were comparable. Rubber trees were planted as rootstock at an initial density of 500 trees ha^{-1}. Root system morphology of these trees has not been measured, but is likely to comprise a taproot with superficial, lateral roots (Masson and Monteuuis, 2017). At the *plantation* site, rubber trees were planted in 2006; mean diameter at breast height (DBH) was 15.4 ± 0.7 cm and mean height was 11.0 ± 4.0 m. At the *clear-cut* site, trees were planted in 1981 and after felling in 2011, stumps were not removed, therefore some root decomposition may have occurred belowground. The different types of vegetation meant that subsurface flow had to be

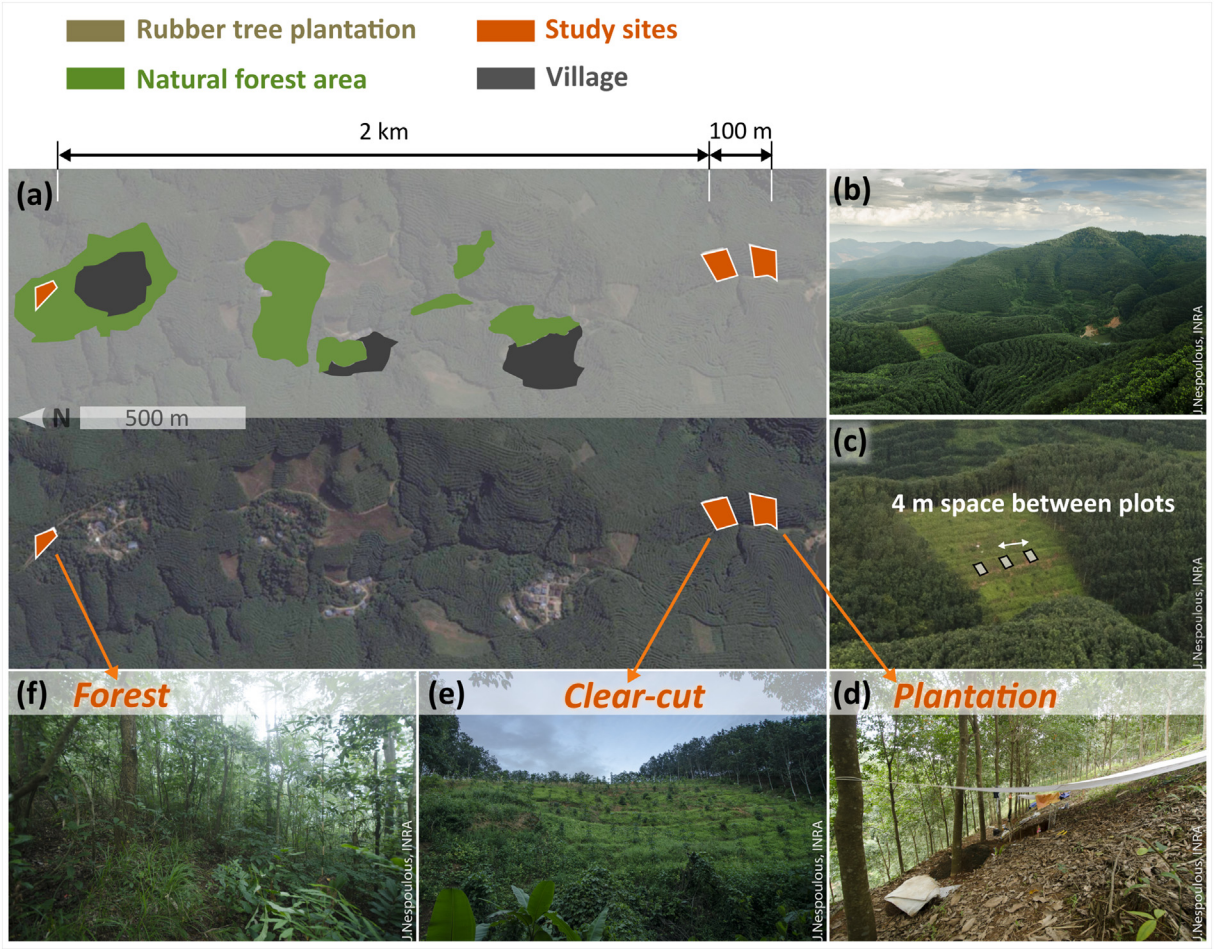

Fig. 1. (a) Forest cover and location of field sites in Nan Lin Shan mountain, Yunnan province (China) (map data: Google, Image ©2015 Digital Globe), (b) general view of the landscape showing the dominance of rubber tree (*Hevea brasiliensis*) plantations and the clear cut site, (c) detail of the location of in situ plots mid-slope in the clear-cut site, (d) rubber tree plantation with bare soil interspersed with litter, (e) clear-cut with understorey grass and (f) mixed secondary forest with diverse understorey strata and litter present.

analysed at the microscale, with a careful analysis of root size and distribution patterns in the soil.

We assessed vegetation composition in three 9 m^2 (3 × 3 m) plots spaced 4 m apart within each of the three sites. In all sites, plots were located mid-slope to avoid changes in topography and slope (i.e. upper and lower parts of the slope with different gradients, Fig. 1c). In the *plantation* and *clear-cut* sites, the centres of the plots were situated 1.5 m upslope of a tree or stump of *H. brasiliensis*. At the *forest* site, plot centres were situated 1.5 m above three different tree species representatives of the natural mixed forest community (*Anthocephalus chinensis* (Lam.) Rich. ex Walp., *Aporosa yunnanensis* (Pax & K.Hoffm.) F. P. Metcalf and *Archidendron monadelphum* (Roxb.) Nielsen var. *monadelphum*, Table 1).

2.3. Soil

Soil analyses were conducted on fractions finer than 2 mm. Percentage sand (2 mm–50 µm), silt (50 µm–2 µm), and clay (< 2 µm) content was determined using the pipette method (NF X31-107, 2003: 31–107). The soil colour of each horizon was determined using a Munsell colour chart (Munsell, 2000). Bulk density measurements were made during the analysis of soil profiles (see Section 2.5, Table S1, Fig. S2).

Soil profiles were similar among sites and were classified as Ferralsols according to the FAO soil classification (IUSS Working Group WRB, 2015) or laterites (oxisols) according to the Chinese and USDA soil classification (Gerasimova, 2010; Soil Survey Staff, 2014). These soils were developed from arenaceous shale sediments (Wang et al., 1996; Cao et al., 2006; Xiao et al., 2014). Soils were described using methodology from FAO (2006) and Soil Science Division Staff (2017). Soil surfaces were covered by a shallow humus layer with fast decomposition classified as "mull" (Graefe et al., 2012). Soils were characterised by a litter layer (O_L) of 0.5 to 0.10 m in *forests* that was absent in *clear-cut* (Fig. 2). The organic decomposed horizon (O_H) was not present as litter as it is quickly mineralised by faunal activity (especially termites). Soils were differentiated by three characteristic soil horizons with gradual and smooth boundaries (Table 2, Fig. 2). An A-horizon was present in the upper 0–0.3 m of soil (*surficial*), characterised by a massive structure with weak to moderate thin granular to blocky peds (FAO, 2006; Soil Science Division Staff, 2017), a clayey texture, a dark yellowish brown colour (Munsell, 2000) and the presence of roots. A B-horizon existed at 0.3–0.6 m deep (*middle*) with less roots, a massive to layered structure with thin blocky peds, a clayey texture and a strong brown colour. A C-horizon was present in the subsoil (0.6–0.8 m - *deep*) with few roots, a massive to layered structure with moderate crumbly peds, clayey texture, a reddish yellow colour and with more gravel and stones at depth, depending on the occurrence of parent rock material. Throughout the profile, soils were slightly moist, acidic (pH = 4.8 ± 0.1) and organic matter content decreased with depth from 4.6% (A-horizon) to 2.7% (B-horizon) to 1.7% (C-horizon).

Table 1
Plant species present at different sites.

Plant species were divided into groups depending on vegetation strata. Tree species present on experimental plots are highlighted in bold. The species names noted sp. and sp2 were identified to the genus level only.

Strata	Species	Family	Mean abundance cover (%)		
			Plantation	*Clear-cut*	*Forest*
Grass	*Ageratum* sp.	Asteraceae			2
	Bambusoideae sp.	Poaceae		30	30
	Crotalaria sp.	Fabaceae		2	2
	Cyclosorus aridus	Thelypteridaceae		13	13
	Cyperus sp.	Cyperaceae		2	2
	Dianella ensifolia	Asphodelaceae		2	2
	Ficus sp.	Moraceae		2	2
	Hedyotis sp.	Rubiaceae		42	
	Hedyotis sp. 2	Rubiaceae		2	2
	Homalanthus sp.	Euphorbiaceae		2	2
	Melastoma sp.	Melastomataceae		2	2
	Microstegium ciliatum	Poaceae		2	2
	Phyllanthus sp.	Phyllanthaceae		10	10
	Pteridium revolutum	Pteridiaceae		2	2
	Rhus chinensis	Anacardiaceae		2	2
	Scleria ciliaris	Cyperaceae		2	2
	Setaria	Poaceae		2	2
	Setaria palmifolium	Poaceae		10	10
	Thysanolaena maxima	Poaceae			2
	Urena lobata	Malvaceae		4	4
Liana	*Lygodium flexuosum*	Lygodiaceae		2	2
Shrub	*Dalbergiia*	Fabaceae			2
	Scleria ciliaris	Cyperaceae			2
	Smilax hypoglauca	Smilacaceae			2
Tree	***Anthocephalus chinensis***	Rubiaceae			11
	Aporosa yunnanensis	Phyllanthaceae			6
	Archidendron monadelphum	Fabaceae, Mimosoideae			6
	Castanopsis mekongensis	Fagaceae			6
	Grewia acuminata	Malvaceae			11
	Hevea brasiliensis	Euphorbiaceae	100	100	
	Syzygium cumini	Myrtaceae			6

2.4. Dye infiltration experiments

The experiments were conducted in August 2014, i.e. during the monsoon season, with a water soil content close to water field capacity. The litter layer was removed and the surface soil water content (0–0.1 m depth) was measured along the border of plots (as described in Section 2.2, before each infiltration experiment), to verify the homogeneity of surface soil moisture between plots for each site. Five surface soil samples per plot were collected and soil moisture measured by the gravimetric method (soils were dried for 48 h at 105 °C (NF ISO 11465, 1994)). *Plantation* plots possessed higher surface soil moisture (49% ± 4%) than the *clear-cut* (34% ± 3%) and *forest* (29% ± 3%) sites. Within each site, no significant differences in soil moisture were found among plots.

Within each plot, we performed one dye infiltration test to visualise the effect of biopores and capture the effects of root systems on flow pathways. Dye infiltration tests have been performed successfully using infiltrometers and irrigation experiments (Noguchi et al., 1997b; Alaoui and Goetz, 2008; Gerke et al., 2015; Clark and Zipper, 2016; Zhang and Xu, 2016). We prepared 60 l of dye, using 480 g of Brilliant Blue FCF powder (a food dye E133 with a relatively low toxicity, low sorption and high mobility (Flury and Fltihler, 1994)), diluted in ordinary tap water (i.e., a concentration of 4 g l^{-1}).

Before irrigation tests, we cut herbaceous plants with scissors at ground level and removed any debris and coarse litter from the soil surface, without disturbing the soil structure. Within each plot, dyed water was irrigated at a distance of 1.5 m upslope of the tree stem (Fig. 3a, b). We chose to apply the dye at this distance to (i) avoid direct flow of dye close and around the stem bole, (ii) to avoid being too close to the upper terrace and (iii) at a distance > 1.5 m, we may not have been able to locate blue dye downslope of the tree. Dye was stored in a tank and applied by pouring it into a 1.0 m long × 0.1 m wide drainpipe perforated with 30 holes (2 mm in diameter). This drainpipe defined the upper limit of a 1.0 m^2 quadrat, which was the focus of further experimental steps and analyses. Dye seeped through the pipe and into the soil at a constant discharge of 10.0 ml s^{-1} (Roose, 1980; Asseline et al., 1993). Discharge was kept relatively constant by keeping water at the same level in the pipe during each test. To promote infiltration, surface runoff was blocked by a metal sheet dam (1.0 m long by 0.08 m deep) 0.3 m downslope of the drainpipe (Fig. 3a, b).

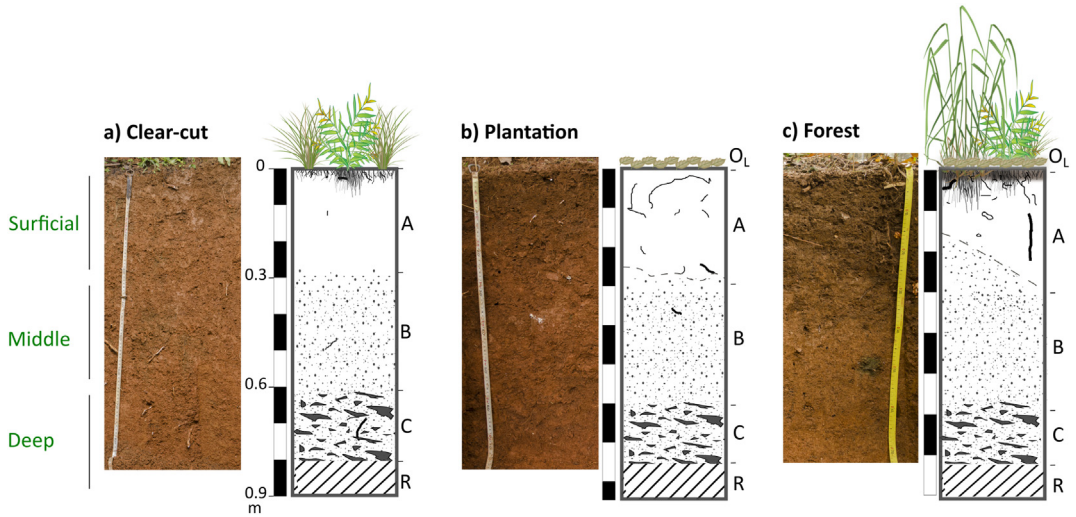

Fig. 2. Typical soil profiles (photograph and schematic drawing) for (a) clear-cut, (b) plantation and (c) forest sites. Soil profiles are described in the Materials and methods section and in Table 2.

Table 2
Soil properties of field sites in Nan Lin Shan.
Textural classification was performed following the USDA soil taxonomy. Data are means ± standard deviation (SD) where appropriate.

Site	Horizon	Depth (m)	Particle size distribution (%)			Texture	Organic matter (%)	pH_{water}	Density (mean ± SD)	Colour (Munsell chart)	Colour
			Sand (2 mm–50 μm)	Silt (50 μm–2 μm)	Clay (< 2 μm)						
Plantation	*A-Surficial*	0–0.3	24.8	31.9	43.3	Clay	3.45	5.28	0.92 ± 0.07	10 YR 4/6	Dark yellowish brown
	B-Middle	0.3–0.6	23.7	32.3	44.0	Clay	2.76	5.18	1.09 ± 0.09	7.5 YR 5/8	Strong brown
	C-Deep	0.6–0.8	27.5	30.7	41.8	Clay	1.69	5.31	NA	7.5 YR 6/8	Reddish yellow
Clear-cut	*A-Surficial*	0–0.3	22.3	31.7	46.0	Clay	4.98	4.66	1.01 ± 0.08	10 YR 4/6	Dark yellowish brown
	B-Middle	0.3–0.6	20.0	39.1	40.9	Clay	2.09	4.70	1.09 ± 0.11	7.5 YR 5/8	Strong brown
	C-Deep	0.6–0.8	24.0	39.8	36.2	Clay loam	1.45	4.48	NA	7.5 YR 6/8	Reddish yellow
Forest	*A-Surficial*	0–0.3	27.3	26.1	46.6	Clay	5.26	4.41	1.06 ± 0.1	10 YR 4/6	Dark yellowish brown
	B-Middle	0.3–0.6	28.0	25.8	46.2	Clay	3.28	4.35	1.22 ± 0.09	7.5 YR 5/8	Strong brown
	C-Deep	0.6–0.8	22.8	25.5	51.7	Clay	1.88	4.61	*NA*	7.5 YR 6/8	Reddish yellow

2.5. Soil profile analysis

After 5 h of infiltration, the soil profile was excavated to bedrock (to a maximum depth of 0.8 m). Soil was carefully removed to produce a smooth profile wall surface, starting from the lower limit of the plot (1.0 m downslope of the irrigation source). A new profile was then made 0.1 m uphill and repeated until 10 soil profiles were excavated. We termed the analysis of these profiles as the "macroscale analysis" that captured the effects of vegetation type on the extension of subsurface flow. To investigate the effects of macrofauna burrows and root size and density on infiltration at the microscale, a 1.0 × 0.8 m grid divided into 0.1 m squares was set in front of each profile (Fig. 4a). Profiles were then photographed to show the intensity and distribution of blue dye for mapping and recording results. Photographs were taken using a digital camera (Nikon D7000–Lens 18–105 f/3.5–5.6: 1/125 s; 5.6 obturator; ISO 200; WB 5500K) situated 1.0 m from each profile on a tripod focused on the centre of the profile. We used a flash (Yongnuo 560II), projected at 45° on a reflector located 1.0 m above the profile and parallel to the slope, to mitigate the brightness differences related to sunshine cycles and forest cover. A neutral grey scale was used to fill and reduce the variability of colour on each photograph.

After each irrigation test, three vertical soil profiles were selected for further analysis: the furthest profile from the drainpipe, where dye was present (thus representing the longest subsurface flow path), and two other profiles, situated at equal distances between the furthest profile with blue dye present and the drainpipe. In these three profiles

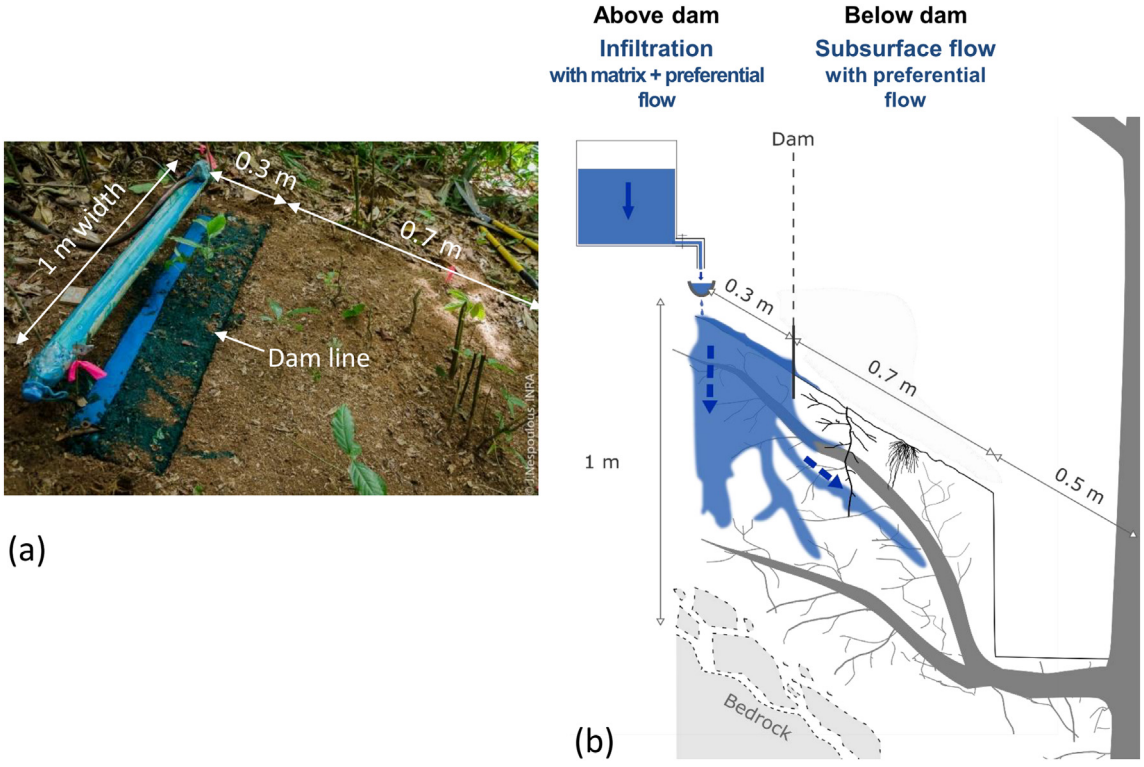

Fig. 3. Brilliant Blue FCF dyed water was applied onto the soil surface at a distance of 1.5 m above the tree stem. (a) Infiltration was performed using a 1 m long pipe with 30 holes (2 mm diameter). Dyed water was applied at a rate of 10 ml s^{-1}. (b) A metal sheet was installed into soil 0.3 m downslope of the pipe to serve as a dam, to avoid excess runoff and promote infiltration. Hydrological processes differed above and below the dam, with a vertical infiltration with matrix flow and preferential flow above the dam and subsurface flow with preferential flow below the dam. (For interpretation of the references to colour in this figure legend, the reader is referred to the web version of this article).

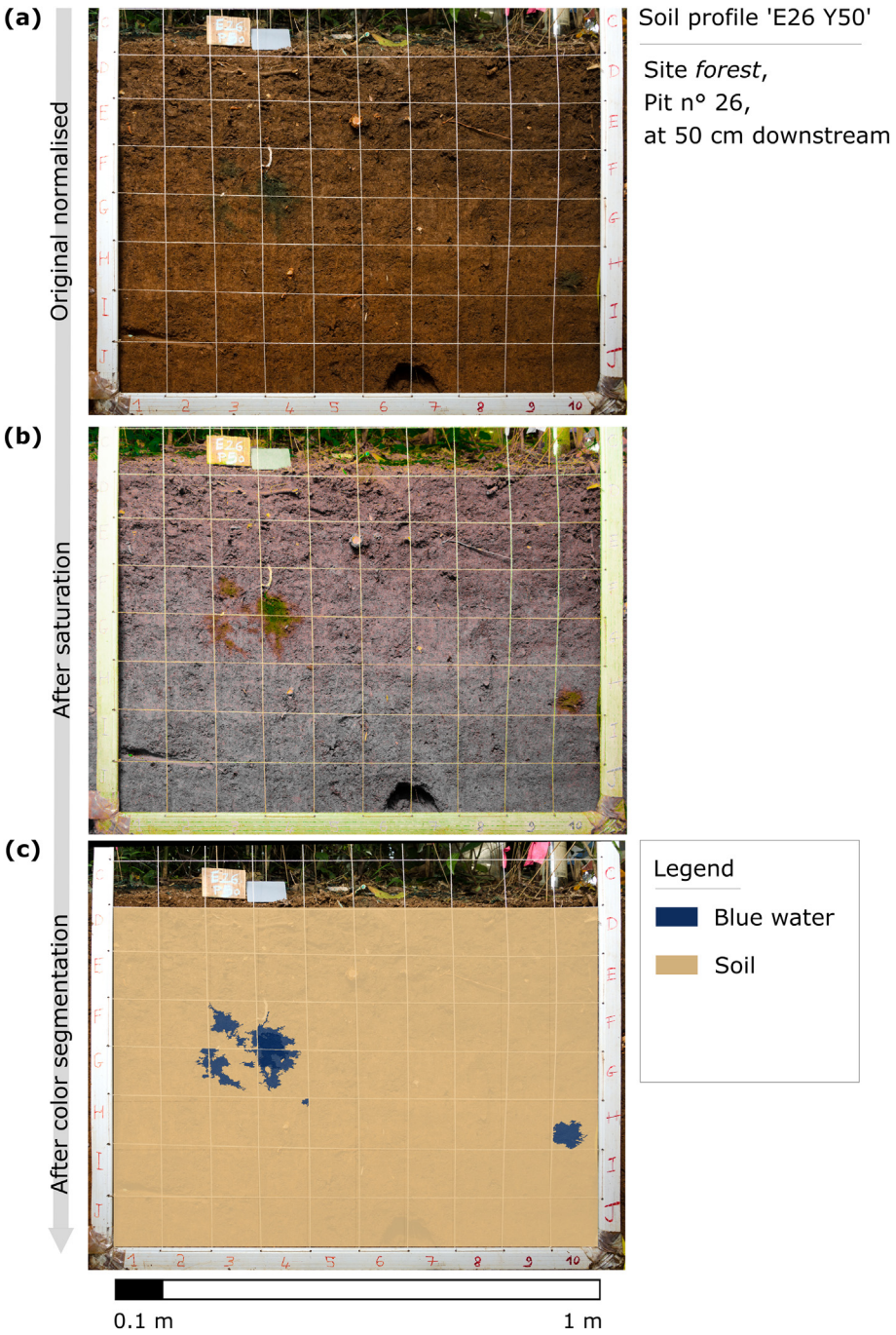

Fig. 4. Image analysis procedure. (a) Soil profile photo recalibrated for colours and luminosity. (b) Soil profile photo normalized after colour saturation. (c) Soil profile image after colour segmentation: colour classes were selected using colour threshold 'object classification.' The blue colour refers to areas stained with Brilliant Blue FCF dyed water. (For interpretation of the references to colour in this figure legend, the reader is referred to the web version of this article).

we measured the root diameter with a calliper and we classed roots into two diameter classes: fine (≤2 mm) and coarse (> 2 mm). In each square, we counted the number of roots present in each class. We distinguished decayed (roots were dark in colour and broke easily) versus not decayed and dyed versus not dyed roots. The presence of biopores generated by soil macrofauna (e.g., termites, ants and worms) such as galleries, cavities, and loosened soil in each cell were visually identified (Supplementary material Fig. S1). In these three soil profiles, we also collected two soil samples from horizons A and B with a sealed cylinder corer (100 cm^3) to measure bulk density (NF X31-501, 1992). A manual sampling of 50 to 100 g of soil was carried out at the same locations and with the addition of the possibility of sampling in horizon C to measure soil water content (Supplementary material Fig. S3, Tables S2, S3). Samples were weighed at field moisture content and then dried in the laboratory for 48 h in an oven at 105 °C and re-weighed (NF ISO 11465, 1994). No significant differences among plots occurred within sites and a general decrease of soil water content with depth was found (Supplementary material Fig. S3, Table S3).

To examine if soil resistance to penetration, and hence compaction, affected subsurface flow, we measured soil resistance using a penetrometer (Humboldt, Dial Pocket Penetrometer H-4205, plunger diameter = 5 mm) in the four corners of each of the 0.1 m squares of the profile. When possible, an additional measurement was added in and at the side of the stained area. From these data we calculated the average

penetration resistance per square. Soil resistance to penetration is generally affected by soil water content. As we did not find significant differences in soil water patterns among plots within sites (Fig. S3, Table S3), the comparisons of soil resistance to penetration were considered as valid.

2.6. Image analysis

The surface area of stained regions was determined from photographs for each selected soil profile. Several steps were necessary in order to obtain data that could quantify the coloured area specifically in relation to depth and intensity of blue colour (Fig. 4). First, we recalibrated colours and luminosity with respect to the neutral grey scale placed on the profile while taking photographs and by de-skewing colour histograms using the Lightroom 6.0 software (Adobe Developer Team, 2016, Fig. 4a). Then, the saturation of the blue stains was maximised to facilitate the differentiation of the dyed intensity. Thus, two main contrasting colours were obtained: green corresponding to blue and grey corresponding to soil (Fig. 4b). We then used the geographic information system program QGIS 2.16 (QGIS Development Team, 2016) to de-skew orthogonally and spatialize the pictures by georeferencing (Geodesic System WGS84; Transverse Universelle the Mercator 31T; polynomial 3 points, nearest neighbours). Finally, we classified colour by using the eCognition 9.0.3 software (eCognition Developer Team, 2016) 'object classification' mode (GIS complementary software) to obtain two classes: 'soil' and 'blue' (Fig. 4c). The shapefile generated by eCognition was imported into Qgis to dissolve polygons by colour classes and intersect them with a referenced spatialized grid to obtain a shapefile with data of area colour classes for each 0.1 m square within a profile. With these data, we could calculate the surface area stained within each 0.1 × 0.1 m square. We did not analyse specific dimensions related to the shape of the dyed areas.

2.7. Data analysis

We analysed data at two scales: i) at the macroscale (1.0 × 0.8 m) to describe how different vegetation types influenced the lateral extension of subsurface flow and ii) at the microscale (in squares of 0.1 × 0.1 m) to describe how the presence of root and macrofauna burrows affect water flow distribution.

At the macroscale, the number of roots per diameter class (< and > 2 mm diameter classes), the presence of fauna, and resistance to penetration were aggregated at three soil depths for each test. These depths corresponded to '*surficial*' (0–0.3 m), which included O and A horizons, '*middle*' (0.3–0.6 m) comprising the B horizon, and '*deep*' (0.6–0.8 m) corresponding to the C horizon. Soil profile depths were different among sites, so the C horizon was not always reached. For the *forest* and *plantation* sites, the C horizon was only present at one and two sites, respectively (Fig. 2). The influence of vegetation type and depth on roots and macrofauna burrows, and resistance to penetration were investigated using Kruskal Wallis and Wilcoxon tests to specify pairwise differences, as data did not follow a normal distribution.

At the microscale, each 0.1 × 0.1 m square was considered a sample. Data from above and below the dam were analysed separately because they were linked to different hydrological processes. Generally, flow was considered 'matrix flow' when a homogeneous wetting front was observed, while 'preferential flow' was when isolated blue dye patches and wetting front instabilities were observed (Cammeraat et al., 2005; Fredlund et al., 2012). We investigated if the subsurface dye distribution was affected by the following factors: (i) depth (in 0.1 m classes from 0 to 0.8 m), (ii) downslope distance from the dye source, (iii) fine and coarse root abundance, and (iv) abundance of faunal burrows. Linear models with mixed effects (LME) were used to identify factors influencing the abundance of the dyed area. As fixed effects, we tested different combinations of factors (fine roots, coarse roots, fauna presence, soil penetration resistance and depth). Plots and soil profiles were considered as random effects and the soil profiles were nested inside the plots. We then selected models with different combinations of the fixed effect predictors by comparing their Akaike Information Criterion (AIC, Burnham and Anderson, 2002) with analysis of variance (ANOVA). At the microscale, we excluded unstained areas from the statistical analysis, because the absence of dye in a cell does not necessarily indicate that the conditions leading to preferential flow are absent, but could be due to different reasons, such as lack of dye to the cell or other preferential flows occurring prior to arrival of dye in the cell. Uniquely focusing on soil cells with the presence of dye (i.e., presence of flow) enables us to ascertain the relationship between roots and macrofauna burrows and dye distribution without noise in the data. Dyed areas detected by the image analyses with a surface area smaller than 0.25 cm^2 were considered as not dyed because they were potentially artefacts related to microtopography, for example microshadows. Statistical analyses were performed using R 3.3.1 (R Core Team, 2016) with the package 'lme4' (Bates et al., 2015) for linear models with mixed effects (LME).

3. Results

3.1. Subsurface flow downslope along the plot and through the profile

A network of biopores comprising channels formed by roots and macrofauna (e.g., termites, ants and earthworms) was visible at every site throughout each soil profile (Fig. S1). Preferential and matrix flows were distinguished by examining the photographs taken for each soil profile. Above the dam, we observed both homogenous matrix and preferential flows, while below the dam we observed preferential flow only, identified as isolated blue patches (Fig. 5). Subsurface flows of dye travelled different distances with depth and along the slope (Fig. 5). Preferential flow often occurred in a zig-zag pattern along a distance of up to 0.9 m in the downslope direction. The maximum horizontal extension of dyed areas differed among sites: flow in *plantation* extended to a mean of 0.50 ± 0.10 m. Flow in *clear cut* extended to a mean of 0.53 ± 0.09 m and in *forest*, flow was found at a mean distance of 0.67 ± 0.15 m. However, the peak of dyed areas (i.e., the profile where the number of cells with the presence of blue dye was greatest) always existed at a distance of 0.10–0.20 m from the dye source, at all sites.

3.2. Effect of vegetation type on biopores

At the macroscale, the *forest* site had a significantly greater number (42 ± 5) of coarse roots (> 2 mm) in the upper 0.3 m of soil, compared to the lower soil depth classes, which were not significantly different from one another (Fig. 6a, $\chi^2 = 4.87$, $P = 0.08$). In the *plantation*, the number of coarse roots was also highest in the uppermost soil layer (11 ± 2) and decreased significantly with depth (Fig. 6a, $\chi^2 = 4.61$, $P = 0.10$). No significant differences were found in coarse root number with any soil depth class at the *clear-cut* site (Fig. 6). Due to the high number of roots in the surficial soil layer at the *forest* site, the mean total number of roots over the entire soil profile was significantly greater than at the *clear-cut* site, but not in the *plantation* (Fig. 6a, $\chi^2 = 6.93$, $P = 0.03$).

At all sites, the number of fine roots (< 2 mm in diameter) was significantly higher in the uppermost soil layer (Fig. 6b, *plantation*: 503 ± 44, $\chi^2 = 6.25$, $P = 0.04$; *clear-cut*: 1261 ± 163, $\chi^2 = 7.20$, $P = 0.02$; *forest*: 918 ± 130, $\chi^2 = 5.14$, $P = 0.07$). The *clear-cut* site with many herbaceous species present, had the greatest number of fine roots in the uppermost soil layer and root numbers decreased significantly with soil depth (Fig. 6b, $\chi^2 = 6.48$, $P = 0.04$). The total mean density of roots in the *forest* site (1292 ± 401 roots m^{-2}) was not significantly greater than in the *plantation* (871 ± 212 roots m^{-2}) or *clear-cut* (1572 ± 566 roots m^{-2}) sites, whereas the latter two sites were significantly different (Fig. 6b, $\chi^2 = 6.49$, $P = 0.04$). With regard

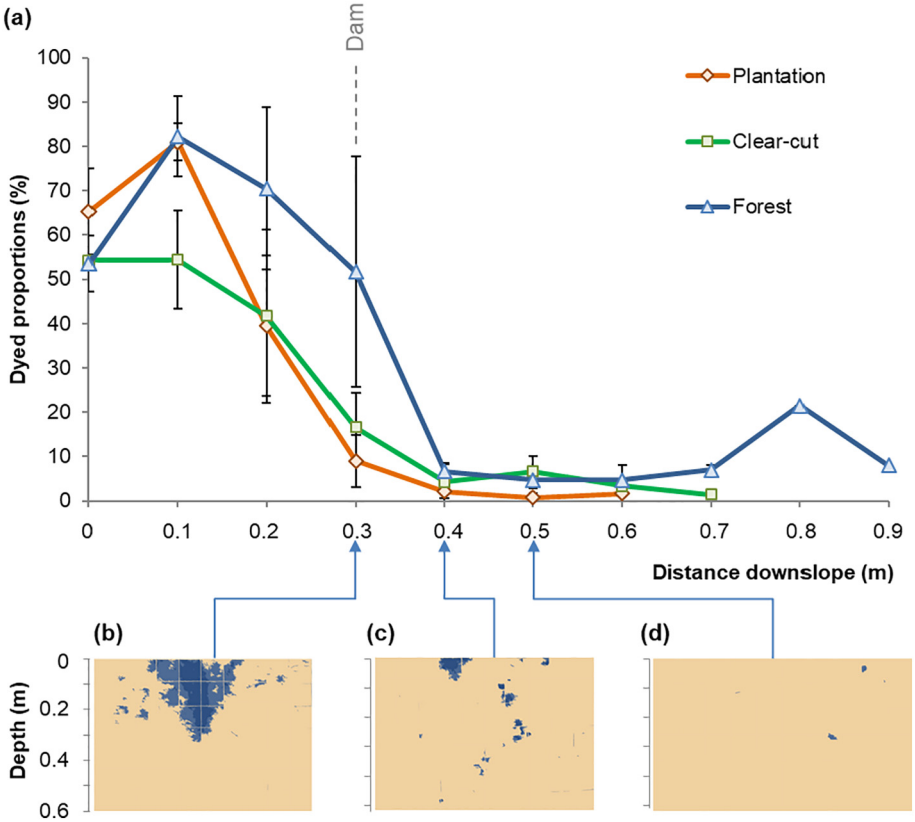

Fig. 5. (a) Mean proportion of surface area stained with Brilliant Blue FCF dyed water flowing downslope along the plot for each site (distance along the slope from the point where dye was applied (0.0 m) and at each subsequent profile every 0.1 m downslope). Data are mean ± standard error. Example of three soil profiles at the plantation site at (b) 0.3 m, (c) 0.4 m and (d) 0.5 m downslope.

to biopores created by macrofauna, no significant differences in the number of biopores were found among soil layers or sites (Fig. 6c).

Soil resistance to penetration ranged from 0 to 12 kPa and increased with increasing depth in the *forest* and *plantation* sites, with the greatest resistance (12 kPa) found in the deepest soil layers of the *forest* site (Fig. 6d, $\chi^2 = 5.14$, $P = 0.07$, compared to the surficial layer (8.4 ± 0.5 kPa) of the *forest* site). Therefore, mean soil resistance over the entire soil profile for the *forest* site was significantly higher (11.1 ± 2.0 kPa) than for the *plantation* site (6.5 ± 1.1 kPa), even though this measurement was also influenced by differences in soil moisture, but not the *clear-cut* site (6.1 ± 0.5 kPa, Fig. 6d, $\chi^2 = 5.95$, $P = 0.05$). No significant differences were found among soil depth classes at the *clear-cut* site.

Bulk density was not significantly different among sites, and for the A horizon was 0.92 ± 0.07 for *plantation*, 1.01 ± 0.08 for *clear-cut*, and 1.06 ± 0.1 for *forest* sites (Table 2). The B horizons were more dense with values ranging from 1.09 ± 0.09 for *plantation* and 1.09 ± 0.11 for *clear-cut* to 1.22 ± 0.09 for *forest*. The deeper horizons were dense and compact but could not be sampled due to their hardness and the high rate of coarse elements (e.g., gravel, pebbles and stones). The variability in bulk density was due mainly to the heterogeneity of the soil structure and affected by the passage of fauna with more or less loose areas between sites (Supplementary material Fig. S2, Table S1).

3.3. Relationships between subsurface flow and biotic factors at the microscale

At the microscale, no significant relationships between the surface area of soil stained with blue dye and number of coarse roots or fauna activity were found either above or below the dam (Fig. S4). Based on LME for dyed cells, above the dam (i.e., matrix and preferential flows), the best fitting model was that including fine root abundance in interaction with site (AIC = 3643, Df = 7, Table 3, Fig. S4). However, below the dam (i.e., preferential flow), the best model included only the abundance of fine roots in interaction with depth (AIC = 1478, Df = 7, Table 3, Fig. S4). Therefore, fine roots were the most important factor affecting dyed areas when compared to coarse roots or faunal channels. At each site, the importance of the presence of fine roots on the dyed area, both above and below the dam, was highlighted when the total dyed area was plotted as a function of fine root presence (Yes vs. No; Fig. 7a, b). For each site, a significant positive linear relationship was found between fine root abundance and dyed area above the dam, although variability in data was high (Fig. 7c). The increment of dyed area due to increasing fine root density was greatest at the *plantation* site (Fig. 7c, Table 3: estimate = 2.77***), intermediate at the *forest* site (Fig. 7c, Table 3: estimate = 2.08***) and smallest at the *clear-cut* site (Fig. 7c, Table 3: estimate = 1.31***). For the data below the dam, the best model included fine roots and interaction with depth (Fig. 6d, Table 3: estimate = 0.99***).

4. Discussion

Subsurface flow and root distribution decreased with depth and distance from source under all types of vegetation. Contrary to our hypothesis, and in all types of vegetation, these results were consistent in terms of the dominant role of fine roots channelling water. We observed differences among sites for both the maximum downslope extension of dyed water flow and the relationship between the dyed area and fine roots. These combined findings highlight the complexity of hydrological processes in soils, at even a local scale.

Each site possessed its own particularities in terms of soil compaction and biotic activities, resulting in disparities of subsurface flow. We found that natural forest had greater downslope subsurface flow propagation than rubber tree plantations, similar to findings from Neris et al. (2012) studying natural evergreen forest and pine (*Pinus canariensis*) plantations and Marín-Castro et al. (2016) investigating secondary tropical montane cloud forest and coffee (*Coffea arabica*)

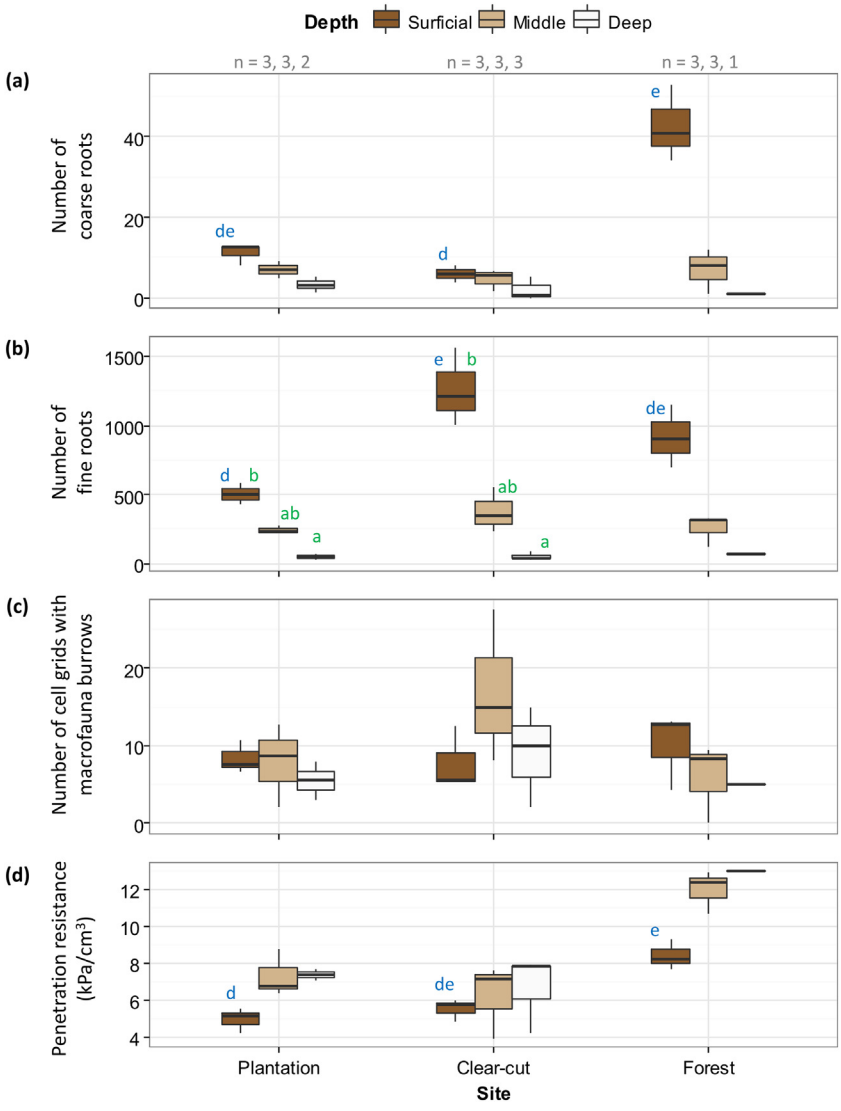

Fig. 6. Soil depth relationships with (a) mean number of coarse roots per horizon per soil profile, (b) mean number of fine roots per horizon soil profile, (c) mean number of cell grids with macrofauna burrows per horizon soil profile and (d) resistance to penetration per horizon soil profile. Data are significantly different ($P < 0.05$) when letters above the boxplots differ. Letters 'a' and 'b' correspond to tests with depth as the factor and letters 'd' and 'e' correspond to tests with site as the factor. If no letters are present, there are no significant differences between factors. The Kruskal-Wallis rank sum test chi-square is the coefficient of determination at the probability level.

Table 3
Estimated parameters for fixed and random effects of selected LMEr explaining the variation of surface area of soil stained with Brilliant Blue FCF dyed water at the microscale: (a) above the dam and (b) below the dam. Estimates are the parameter estimates with σ standing for standard deviation for random effects. Std. Err are the standard errors of the estimates. t represents the ratio of estimates and their standard errors, and P is the associated probability value from a t distribution.

Groups	Estimate	Std. err.	df	t	P
a) Above dam (Y < 0.3 m)					
(Intercept)	17.01	2.82	15.13	6.03	< 0.001
Fine roots: Site plantation	2.77	0.29	102.70	9.52	< 0.001
Fine roots: Site forest	2.08	0.24	256.71	8.72	< 0.001
Fine roots: Site clear-cut	1.31	0.16	223.17	8.36	< 0.001
b) Below dam (Y > 0.3 m)					
(Intercept)	9.54	3.28	72.85	2.91	< 0.01
Fine roots	0.99	0.40	173.25	2.47	< 0.05
Depth	−0.15	0.07	178.76	2.10	< 0.05
Fine roots: Depth	0.05	0.02	177.63	3.02	< 0.01

plantations. Bodhinayake and Cheng Si (2004) also showed that greater preferential flow occurred in flat grasslands compared to cultivated soils. Other authors demonstrated higher preferential flows on sites with trees than in grasslands (Joffre and Rambal, 1988; Belsky et al., 1993; van Schaik, 2009; Perkins et al., 2012) or beneath trees in agroforests (Wang and Zhang, 2017). In agreement with Zhu et al. (2018), we show that converting natural forest to plantations may induce an increase of runoff due to a decrease of infiltration and subsurface flow. This impact would be significantly reduced if monocropped plantations were converted to e.g., alley cropping (Sun et al., 2018).

We showed that coarse root abundance was significantly greater in the upper 0.3 m of soil in the *forest* site, compared to soil (shallow or deep) of any site, probably due to the greater diversity and density of trees along the slope. Increasing species diversity will lead to a greater number of root system morphologies and hence a more enhanced spatial occupation of the soil profile (Stokes et al., 2009). Although we did not measure litter properties, enhanced litter thickness in natural forests also increases hydraulic conductivity compared to plantation forests (Marín-Castro et al., 2017). The greatest abundance of fine roots (< 2 mm in diameter) was near the soil surface in the *clear-cut* site, with many herbaceous species present, resulting in a higher subsurface flow propagation in the top 0.3 m of soil, as also found by Bodhinayake and Cheng Si (2004).

With regard to biopores created by soil fauna, surprisingly, we did not see significant differences among soil layers and sites. Léonard and Rajot (2001) also discussed the difficulty in quantifying the effect of termites on runoff and infiltration because data were highly variable.

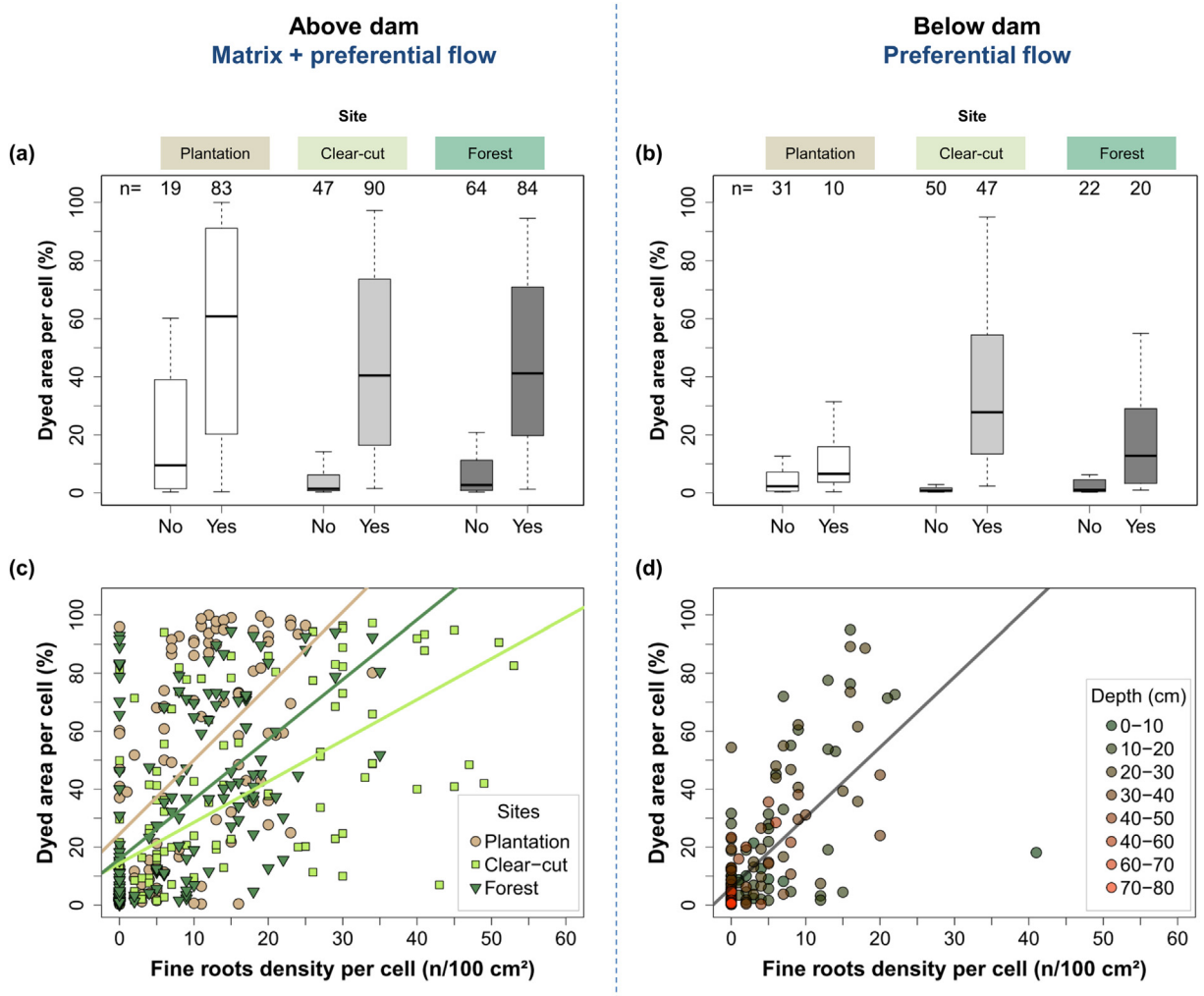

Fig. 7. Relationships between the soil surface area of blue dye and fine roots. Boxplot comparing the blue dye distribution in terms of fine root absence (No) or presence (Yes) at a) above the dam and b) below the dam. Scatterplot showing dyed area in relation to c) the number of fine roots, with site highlighted with different colours above the dam in which trends are $y_{plantation} = 2.55\ x + 24.50$, $P < 0.001$, $R^2 = 0.29$, $y_{clear\text{-}cut} = 1.41\ x + 14.40$, $P < 0.001$, $R^2 = 0.41$, $y_{forest} = 2.06\ x + 15.95$, $P < 0.001$, $R^2 = 0.33$ and (d) below the dam with depth highlighted with different colours in which the general trend is $y = 2.42\ x + 6.02$, $P < 0.001$, $R^2 = 0.46$. Trends are obtained from linear models between $\%_{dyed\ surface\ area}$ and the number of fine roots. (For interpretation of the references to colour in this figure legend, the reader is referred to the web version of this article).

These authors found a significant effect of fauna that increased infiltration and reduced runoff (also shown by Beven and Germann, 1982; Capowiez et al., 2012; Cheng et al., 2017; Schneider et al., 2018), and Jouquet et al. (2012) showed that macrofaunal activity reduced soil erosion on a fallow slope in Vietnam. Soil resistance to penetration increased with depth in *forest* and *plantation* sites, with the greatest resistance found in the deepest soil layers of the *forest* site. *Forest* had different soil physical properties than those of the *plantation* sites (in which the soil structure was possibly affected by terrace construction). The changes in slope geometry in terraced terrain can affect subsurface flow and alter the position of the wetting front (Cammeraat et al., 2005; Sidle et al., 2006).

We highlighted the positive effect of biological activity on subsurface flow. For each of the three sites, we demonstrated that live, fine roots had a more dominant effect on subsurface flow compared to coarse roots and soil fauna, contrary to our initial hypothesis. This finding shows the importance of considering the multiple roles of fine roots when studying the soil-plant-water continuum. Fine roots, which grow fast and are usually more numerous than thicker roots, may make, in a short time, many non-capillary channels that can greatly improve the soil infiltration capacity. Also, fine roots should be more susceptible to soil dryness and thus more prone to root shrinkage that create gaps between the root and the soil (DeRoo, 1968). Fine roots also have a very fast turnover rate (30 to 1000 days) and thus form dead root channels more quickly than coarse roots that remain longer in the soil (McCormack and Guo, 2014; McCormack et al., 2015; Germon et al., 2015). These processes are also beneficial for enhancing soil infiltration capacity.

Although we demonstrated that the potential effect of land-use changes on preferential flow was related to variations in the density and size of biopores, our field sites were not replicated at the forest or watershed scale, therefore, it is difficult to extrapolate results beyond the scale of individual trees. To understand infiltration and subsurface flow processes at a greater scale, it would be necessary to perform more numerous and simpler infiltration tests, or larger-scale assessments of infiltration. Nevertheless, our study contributes to the increasing number of studies showing that subsurface flow and especially preferential flow, increase water drainage, thereby reducing surficial runoff and erosion processes. Preferential flow can also reduce the build-up of pore water pressure within soil, and so decrease the triggering of rainfall induced landslides (but adverse effects are also possible, see Ghestem et al., 2011). Therefore, our results suggest that mixtures of species should protect against soil erosion and possibly slope instability. In cultivated soils, tree and shrubby/herbaceous

mixtures, such as alley cropping (Jiang et al., 2017), or no- or soft-intercropping weeding (Liu et al., 2019), would be beneficial for soil conservation.

5. Conclusion

We studied subsurface flow processes at the microscale (corresponding to individual biopores, roots and fauna) and the macro-scale (corresponding to the soil profile around individual trees). Our results show the complexity of the drivers of preferential flow in soils. The role of fine roots promoting subsurface flow was dominant over macrofaunal burrows and coarse roots. The consistent positive relationship between fine root density and subsurface flow can help to support assumptions of the effects of roots on rapid drainage during an intense rain event. This drainage should efficiently reduce surface runoff and surface erosion during heavy rainfall and promote downslope drainage, which can have beneficial or adverse effects on slope stability. These results demonstrate the need to consider using species mixtures in local forest conversion programs to avoid mass wasting processes and soil erosion, e.g. agroforestry, alley-cropping systems or plantations with understorey species present.

Declaration of interest

The authors declare that they have no competing interests.

Acknowledgements

Funding was jointed provided by the BMU (Germany) International Climate Initiative funded project 'Ecosystems protecting infrastructure and communities' (11_II + _005_A_EPIC), a Campus France Xuguangqi program "IMMORTEL" (Interactions between biomechanical and morphological root traits and their impact on soil erosion and landslide mitigation, XGC - 34442WB) and an INRA PhD demi-bursary (JN). Thanks are due to XTBG, Eric Leveque and villagers for logistic help. We are grateful to, Gilles Le Moguedec (INRA France), Pierre Honoré (Photographer), Kyle Tomlinson (CAS, China), Yan Wang (CAS, China), Tristan Charles-Dominique (CNRS, France) and Don Picker (IASHK, Hong Kong) for help with data analysis, soil photographic protocol management and species' identification.

Appendix A. Supplementary data

Supplementary data to this article can be found online at https://doi.org/10.1016/j.catena.2019.05.007.

References

Adobe Developer Team, 2016. Adobe Photoshop Lightroom. Adobe System Incorporated.
Ahrends, A., Hollingsworth, P.M., Ziegler, A.D., Fox, J.M., Chen, H., Su, Y., Xu, J., 2015. Current trends of rubber plantation expansion may threaten biodiversity and livelihoods. Glob. Environ. Chang. 34, 48–58.
Alaoui, A., 2006. Estimation du flux dans la zone non saturée. Méthode simple - Connaissance de l'environnement. Office fédéral de l'environnement (OFEV) (UW-0702-F) 52.
Alaoui, A., Goetz, B., 2008. Dye tracer and infiltration experiments to investigate macropore flow. Geoderma, Antarctic Soils and Soil Forming Processes in a. Changing Environment 144 (1–2), 279–286.
Asseline, J., De Noni, G., Nouvelot, J.-F., Roose, E., 1993. Note sur la conception et l'utilisation d'un simulateur de ruissellement. Cahiers ORSTOM. Série Pédologie 28 (2), 405–411.
Aubertin, G., 1971. Nature and Extent of Macropores in Forest Soils and Their Influence on Subsurface Water Movement. Research Paper NE-192 USDA Forest Service, pp. 33.
Bates, D., Mächler, M., Bolker, B., Walker, S., 2015. Fitting linear mixed-effects models using lme4. J. Stat. Softw. 67.
Belsky, A.J., Mwonga, S.M., Amundson, R.G., Duxbury, J.M., Ali, A.R., 1993. Comparative effects of isolated trees on their undercanopy environments in high- and low-rainfall savannas. J. Appl. Ecol. 30 (1), 143.
Bengough, A.G., Croser, C., Pritchard, J., 1997. A biophysical analysis of root growth under mechanical stress. Plant Soil 189 (1), 155–164.
Beven, K., Germann, P., 1982. Macropores and water flow in soils. Water Resour. Res. 18, 1311–1325.
Bodhinayake, W., Cheng Si, B., 2004. Near-saturated surface soil hydraulic properties under different land uses in the St Denis National Wildlife Area, Saskatchewan, Canada. Hydrol. Process. 18 (15), 2835–2850.
Bodner, G., Leitner, D., Kaul, H.-P., 2014. Coarse and fine root plants affect pore size distributions differently. Plant Soil 1–19.
Bormann, H., Klaassen, K., 2008. Seasonal and land use dependent variability of soil hydraulic and soil hydrological properties of two Northern German soils. Geoderma, Modelling Pedogenesis 145 (3–4), 295–302.
Burnham, K.P., Anderson, D.R., 2002. Model Selection and Multimodel Inference: A Practical Information-Theoretic Approach, 2nd ed. Springer.
Cammeraat, E., van Beek, R., Kooijman, A., 2005. Vegetation succession and its consequences for slope stability in SE Spain. Plant Soil 278 (1), 135–147.
Cao, M., Zou, X., Warren, M., Zhu, H., 2006. Tropical forests of Xishuangbanna, China. Biotropica 38 (3), 306–309.
Capowiez, Y., Samartino, S., Cadoux, S., Bouchant, P., Richard, G., Boizard, H., 2012. Role of earthworms in regenerating soil structure after compaction in reduced tillage systems. Soil Biol. Biochem. 55, 93–103.
Cheng, Y., Ogden, F.L., Zhu, J., 2017. Earthworms and tree roots: a model study of the effect of preferential flow paths on runoff generation and groundwater recharge in steep, saprolitic, tropical lowland catchments. Water Resour. Res. 53, 5400–5419.
Clark, E.V., Zipper, C.E., 2016. Vegetation influences near-surface hydrological characteristics on a surface coal mine in eastern USA. Catena 139, 241–249.
DeRoo, H.C., 1968. Tillage and root growth. In: Whittington, W.J. (Ed.), Root Growth. Butterworths, London, pp. 339–358.
eCognition Developer Team, 2016. eCognition. Trimble.
Elkin, C., Gutiérrez, A.G., Leuzinger, S., Manusch, C., Temperli, C., Rasche, L., Bugmann, H., 2013. A 2 °C warmer world is not safe for ecosystem services in the European Alps. Glob Change Biol 19 (6), 1827–1840.
FAO, 2006. Guidelines for Soil Description, 4th ed. (Rome).
Farenhorst, A., Topp, E., Bowman, B.T., Tomlin, A.D., 2000. Earthworm burrowing and feeding activity and the potential for atrazine transport by preferential flow. Soil Biol. Biochem. 32 (4), 479–488.
Flury, M., Fltihler, H., 1994. Brilliant Blue FCF as a dye tracer for solute transport studies - a toxicological overview. J. Environ. Qual. 23 (5).
Fredlund, D.G., Rahardjo, H., Fredlund, M.D., 2012. Unsaturated Soil Mechanics in Engineering Practice: Fredlund/Unsaturated Soil Mechanics. John Wiley & Sons, Inc., Hoboken, NJ, USA.
Gerasimova, M.I., 2010. Chinese soil taxonomy: between the American and the international classification systems. Eurasian Soil Sci. 43 (8), 945–949.
Gerke, K.M., Sidle, R.C., Mallants, D., 2015. Preferential flow mechanisms identified from staining experiments in forested hillslopes. Hydrol. Process. 29, 4562–4578.
Germon, A., Cardinael, R., Prieto, I., Mao, Z., Kim, J., Stokes, A., Dupraz, C., Laclau, J.-P., Jourdan, C., 2015. Unexpected phenology and lifespan of shallow and deep fine roots of walnut trees grown in a silvoarable Mediterranean agroforestry system. Plant Soil 401 (1–2), 409–426.
Ghestem, M., Sidle, R.C., Stokes, A., 2011. The influence of plant root systems on subsurface flow: implications for slope stability. BioScience 61 (11), 869–879.
Graefe, U., Baritz, R., Broll, G., Kolb, E., Milbert, G., Wachendorf, C., 2012. Adapting Humus Form Classification to WRB Principles.
Häuser, I., Martin, K., Germer, J., He, P., Blagodatsky, S., Liu, H., Krauß, M., Rajaona, A., Min, S., Pelz, S., Langenberger, G., Zhu, C.-D., Cotter, M., Stuerz, S., Waibel, H., Steinmetz, H., Wieprecht, S., Frör, O., Ahlheim, M., Cadisch, G., 2015. Environmental and socio-economic impacts of rubber cultivation in the Mekong region: challenges for sustainable land use. CAB Reviews: Perspectives in Agriculture, Veterinary Science, Nutrition and Natural Resources 10 (27), 1–11.
IUSS Working Group WRB, 2015. World Reference Base for soil resources 2014, update 2015 international soil classification system for naming soils and creating legends for soil maps. In: World Soil Resources Reports. No. 106. FAO, Rome.
Jiang, X.J., Liu, W., Wu, J., Wang, P., Liu, C., Yuan, Z.-Q., 2017. Land degradation controlled and mitigated by rubber-based agroforestry systems through optimizing soil physical conditions and water supply mechanisms: a case study in Xishuangbanna, China. Land Degrad. Dev. 28, 2277–2289.
Jiang, X.J., Liu, W., Chen, C., Liu, J., Yuan, Z.-Q., Jin, B., Yu, X., 2018. Effects of three morphometric features of roots on soil water flow behavior in three sites in China. Geoderma 320, 161–171.
Joffre, R., Rambal, S., 1988. Soil water improvement by trees in the rangelands of southern Spain. Acta oecologica. Oecologia Plantarum 9 (4), 405–422.
Jouquet, P., Janeau, J.-L., Pisano, A., Sy, H.T., Orange, D., Minh, L.T.N., Valentin, C., 2012. Influence of earthworms and termites on runoff and erosion in a tropical steep slope fallow in Vietnam: a rainfall simulation experiment. Appl. Soil Ecol. 61, 161–168.
Lange, B., Lüescher, P., Germann, P.F., 2009. Significance of tree roots for preferential infiltration in stagnic soils. Hydrol. Earth Syst. Sci. 13, 1809–1821.
Léonard, J., Rajot, J.L., 2001. Influence of termites on runoff and infiltration: quantification and analysis. Geoderma 104, 17–40.
Liu, W., Luo, Q., Li, J., Wang, P., Lu, H., Liu, W., Li, H., 2015. The effects of conversion of tropical rainforest to rubber plantation on splash erosion in Xishuangbanna, SW China. Hydrol. Res. 46 (1), 168.
Liu, H., Yang, X., Blagodatsky, S., Marohn, C., Liu, F., Xu, J., Cadisch, G., 2019. Modelling weed management strategies to control erosion in rubber plantations. Catena 172, 345–355.
Marín-Castro, B.E., Geissert, D., Negrete-Yankelevich, S., Gómez-Tagle Chávez, A., 2016. Spatial distribution of hydraulic conductivity in soils of secondary tropical montane cloud forests and shade coffee agroecosystems. Geoderma 283, 57–67.
Marín-Castro, B.E., Negrete-Yankelevich, S., Geissert, D., 2017. Litter thickness, but not

root biomass, explains the average and spatial structure of soil hydraulic conductivity in secondary forests and coffee agroecosystems in Veracruz, Mexico. Sci. Total Environ. 607–608, 1357–1366.
Masson, A., Monteuuis, O., 2017. Rubber tree clonal plantations: grafted vs self-rooted plant material. Bois et Forêts des Tropiques 332, 57–68.
McCormack, M.L., Guo, D., 2014. Impacts of environmental factors on fine root lifespan. Front. Plant Sci. 5.
McCormack, M.L., Dickie, I.A., Eissenstat, D.M., Fahey, T.J., Fernandez, C.W., Guo, D., Helmisaari, H.-S., Hobbie, E.A., Iversen, C.M., Jackson, R.B., Leppälammi-Kujansuu, J., Norby, R.J., Phillips, R.P., Pregitzer, K.S., Pritchard, S.G., Rewald, B., Zadworny, M., 2015. Redefining fine roots improves understanding of below-ground contributions to terrestrial biosphere processes. New Phytol. 207 (3), 505–518.
Mitchell, A.R., Ellsworth, T.R., Meek, B.D., 1995. Effect of root systems on preferential flow in swelling soil. Commun. Soil Sci. Plant Anal. 26 (15–16), 2655–2666.
Munsell Color Company, 2000. Munsell Soil Color Charts: Year 2000 Revised Washable Edition.
Neris, J., Jiménez, C., Fuentes, J., Morillas, G., Tejedor, M., 2012. Vegetation and land-use effects on soil properties and water infiltration of Andisols in Tenerife (Canary Islands, Spain). Catena 98, 55–62.
NF ISO 11465, 1994. Qualité du sol - Détermination de la teneur pondérale en matière sèche et en eau - Méthode gravimétrique. Afnor, Paris.
NF X31-107, 2003. Qualité du sol - Détermination de la distribution granulométrique des particules du sol - Méthode à la pipette. Afnor, Paris.
Noguchi, S., Rahim Nik, A., Kasran, B., Tani, M., Sammori, T., Morisada, K., 1997a. Soil physical properties and preferential flow pathways in tropical rain forest, Bukit Tarek, Peninsular Malaysia. J. For. Res. 2 (2), 115–120.
Noguchi, S., Tsuboyama, Y., Sidle, R.C., Hosoda, I., 1997b. Spatially distributed morphological characteristics of macropores in forest soils of Hitachi Ohta Experimental Watershed, Japan. J. For. Res. 2 (4), 207–215.
Noguchi, S., Tsuboyama, Y., Sidle, R.C., Hosoda, I., 1999. Morphological characteristics of macropores and the distribution of preferential flow pathways in a forested slope segment. Soil Sciences Society of America Journal 63 (5), 1413–1423.
Noguchi, S., Tsuboyama, Y., Sidle, R.C., Hosoda, I., 2001. Subsurface runoff characteristics from a forest hillslope soil profile including macropores, Hitachi Ohta, Japan. Hydrol. Process. 15 (11), 2131–2149.
Perkins, K.S., Nimmo, J.R., Medeiros, A.C., 2012. Effects of native forest restoration on soil hydraulic properties, Auwahi, Maui, Hawaiian Islands. Geophys. Res. Lett. 39 (L05405).
QGIS Development Team, 2016. QGIS Geographic Information System. Open Source Geospatial Foundation Project.
R Core Team, 2016. R: A Language and Environment for Statistical Computing. R Foundation for Statistical Computing, Vienna, Austria.
Roose, E., 1980. Dynamique actuelle d'un sol ferrallitique sablo-argileux très désaturé sous cultures et sous forêt dense humide sub-équatoriale du Sud de la Côte d'Ivoire: Adiopodoumé 1964–1975 (No. 86). ORSTOM, Paris, France.
Schneider, A.-K., Hohenbrink, T.L., Reck, A., Zangerlé, A., Schröder, B., Zehe, E., van Schaik, L., 2018. Variability of earthworm-induced biopores and their hydrological effectiveness in space and time. Pedobiologia 71, 8–19.
Schwartz, R.C., Evett, S.R., Unger, P.W., 2003. Soil hydraulic properties of cropland compared with reestablished and native grassland. Geoderma, Quantifying agricultural management effects on soil properties and processes 116 (1–2), 47–60.
Shuster, W., Subler, S., McCoy, E., 2002. The influence of earthworm community structure on the distribution and movement of solutes in a chisel-tilled soil. Appl. Soil Ecol. 21 (2), 159–167.
Sidle, R.C., Bogaard, T.A., 2016. Dynamic earth system and ecological controls of rainfall-initiated landslides. Earth Sci. Rev. 159, 275–291.
Sidle, R.C., Ochiai, H., 2006. Landslides: Processes, Prediction, and Land Use, Water Resources Monograph. American Geophysical Union, Washington, DC.
Sidle, R.C., Noguchi, S., Tsuboyama, Y., Laursen, K., 2001. A conceptual model of preferential flow systems in forested hillslopes: evidence of self-organization. Hydrol. Process. 15 (10), 1675–1692.
Sidle, R.C., Ziegler, A.D., Negishi, J.N., Nik, A.R., Siew, R., Turkelboom, F., 2006. Erosion processes in steep terrain-truths, myths, and uncertainties related to forest management in Southeast Asia. For. Ecol. Manag. 224 (1–2), 199–225.
Sidle, R.C., Ghestem, M., Stokes, A., 2014. Epic landslide erosion from mountain roads in Yunnan, China – challenges for sustainable development. Natural Hazards and Earth System Science 14 (11), 3093–3104.
Sidle, R.C., Gomi, T., Loaiza Usuga, J.C., Jarihani, B., 2017. Hydrogeomorphic processes and scaling issues in the continuum from soil pedons to catchments. Earth Sci. Rev. 175, 75–96.
Soil Science Division Staff, 2017. Examination and description of soil profiles. In: Ditzler, C., Scheffe, K., Monger, H.C. (Eds.), Soil Survey Manual. USDA Handbook 18 Government Printing Office, Washington, D.C, pp. 83–268.
Soil Survey Staff, 2014. Keys to Soil Taxonomy (No. 12). Natural Resources Conservation Service, United States Department of Agriculture, Washington, D.C.
Stokes, A., Atger, C., Bengough, A.G., Fourcaud, T., Sidle, R.C., 2009. Desirable plant root traits for protecting natural and engineered slopes against landslides. Plant Soil 324, 1–2), 1–30.
Stokes, A., Sotir, R., Chen, W., Ghestem, M., 2010. Soil bio- and eco-engineering in China: past experience and future priorities. Ecol. Eng. 36 (3), 247–257.
Stokes, A., Raymond, P., Polster, D., Mitchell, S.M., 2013. Engineering the ecological mitigation of hillslope stability research into the scientific literature. Ecol. Eng. 61, 615–620 part C.
Sun, D., Yang, H., Guan, D., Yang, M., Wu, J., Yuan, F., Jin, C., Wang, A., Zhang, Y., 2018. The effects of land use change on soil infiltration capacity in China: a meta-analysis. Sci. Total Environ. 626, 1394–1401.
Tsuboyama, Y., Sidle, R.C., Noguchi, S., Hosoda, I., 1994. Flow and solute transport through the soil matrix and macropores of a hillslope segment. Water Resour. Res. 30 (4), 879–890.
Tsukamoto, Y., Ohta, T., 1988. Runoff process on a steep forested slope. Journal of Hydrology, Hydrologic Research: The U.S. — Japan Experience 102, 165–178.
van Dijk, A.I.J.M., 2002. Water and Sediment Dynamics in Bench-terraced Agricultural Steeplands in West Java, Indonesia. Free University, Amsterdam.
van Schaik, N.L.M.B., 2009. Spatial variability of infiltration patterns related to site characteristics in a semi-arid watershed. Catena 78 (1), 36–47.
Vogel, H.-J., Cousin, I., Ippisch, O., Bastian, P., 2006. The dominant role of structure for solute transport in soil: experimental evidence and modelling of structure and transport in a field experiment. Hydrol. Earth Syst. Sci. Discuss. 10 (4), 495–506.
Wang, W.F., Qiu, D.Y., Wu, J.C., Wu, H.M., 1996. The Soils of Yunnan. Yunnan Science and Technology Press, Kunming.
Wang, Y., Zhang, B., 2017. Chapter Four - Interception of Subsurface Lateral Flow Through Enhanced Vertical Preferential Flow in an Agroforestry System Observed Using Dye-Tracing and Rainfall Simulation Experiments. In: Banwart, S.A., Sparks, D.L. (Eds.), Advances in Agronomy, Quantifying and Managing Soil Functions in Earth's Critical Zone. Academic Press, pp. 99–118. https://doi.org/10.1016/bs.agron.2016.10.014.
Weiler, M., Naef, F., 2003. An experimental tracer study of the role of macropores in infiltration in grassland soils. Hydrol. Process. 17 (2), 477–493.
Wu, G.-L., Liu, Y., Yang, Z., Cui, Z., Deng, L., Chang, X.-F., Shi, Z.-H., 2017. Root channels to indicate the increase in soil matrix water infiltration capacity of arid reclaimed mine soils. J. Hydrol. 546, 133–139.
X31-501, N.F., N.F., 1992. Qualité des sols - Méthodes physiques - Mesure de la masse volumique apparente d'un échantillon de sol non remanié - Méthode du cylindre. Afnor, Paris.
Xiao, H.F., Tian, Y.H., Zhou, H.P., Ai, X.S., Yang, X.D., Schaefer, D.A., 2014. Intensive rubber cultivation degrades soil nematode communities in Xishuangbanna, southwest China. Soil Biol. Biochem. 76, 161–169.
Zhang, J., Xu, Z., 2016. Dye tracer infiltration technique to investigate macropore flow paths in Maka Mountain, Yunnan Province, China. J. Cent. South Univ. 23 (8), 2101–2109.
Zhang, J., Lei, T., Qu, L., Chen, P., Gao, X., Chen, C., Yuan, L., Zhang, M., Su, G., 2017. Method to measure soil matrix infiltration in forest soil. J. Hydrol. 552, 241–248.
Zhu, X., Liu, W., Jiang, X.J., Wang, P., Li, W., 2018. Effects of land-use changes on runoff and sediment yield: implications for soil conservation and forest management in Xishuangbanna, Southwest China. Land Degrad. Dev. 29, 2962–2974.
Ziegler, A.D., Fox, J.M., Xu, J., 2009. The rubber juggernaut. Science 324 (5930), 1024–1025.